American Journal of Mechanical Engineering, 2016, Vol. 4, No. 2, 42-49
Available online at http://pubs.sciepub.com/ajme/4/2/1

DOI:10.12691/ajme-4-2-1

Numerical Investigation of the Transient Radiative Heat Transfer inside a Hexagonal Furnace Filled with Particulate Medium

Elham Khademi Moghadam[1,*], Rasool Nasr Isfahani[2], Arash Azimi[3]

[1]Department of Physics, Shahid Chamran University of Ahvaz, Ahvaz, Iran
[2]Department of Mechanical and Aerospace Engineering, University of Florida, Gainesville, FL 32611, USA
[3]Department of Mechanical and Aerospace Engineering, Islamic Azad University, Tehran 14778-93855, Iran
*Corresponding author: ekhmoghadam@gmail.com

Abstract The transient radiative heat transfer in two 2D irregular geometry filled with particulate media is numerically investigated. The radiative transfer equation is solved with FTn finite volume method. Non-orthogonal mesh is used to discretize the computational domain and the high resolution CLAM scheme is utilized to relate the facial intensities to the nodal values. Various cases of scattering in media with real indices of refraction (dielectric particles) and complex indices of refraction (absorbing particles) are considered. Both Mie theory and equivalent isotropic approximation are used to account for the scattering behavior of the media. The difference between these two methods is found insignificant, especially for the steady state solutions and for media with complex indices of refraction, while the complexity and computational cost of the equivalent isotropic approximation is much lower than those of Mie theory.

Keywords: *transient radiative heat transfer, Mie Theory, equivalent isotropic approximation, finite volume method, non-orthogonal grid*

Cite This Article: Elham Khademi Moghadam, Rasool Nasr Isfahani, and Arash Azimi, "Numerical Investigation of the Transient Radiative Heat Transfer inside a Hexagonal Furnace Filled with Particulate Medium." *American Journal of Mechanical Engineering*, vol. 4, no. 2 (2016): 42-49. doi: 10.12691/ajme-4-2-1.

1. Introduction

The transient radiative transfer finds applications in many emerging technologies such as short pulsed laser in turbid media, remote sensing, nondestructive biomedical diagnosis and combustion product analysis. The transient radiative transfer equation (TRTE) must be solved to find the radiative intensity field.

Thus far, most of the proposed methods for solving the radiative transfer equation (RTE) are extended to solve TRTE. Among these various methods, finite volume method (FVM) has been a favorite to the researchers due to its merits such as being easily programmable, fairly accurate and computationally cheap [1-17]. Chai [1,10] and Chai et al. [2] have applied FVM to solve TRTE. They numerically investigated radiative transfer in 1-, 2- and 3D systems containing the emitting, absorbing and anisotropically scattering media. They also compared the results obtained by STEP scheme with those of CLAM scheme and concluded that CLAM scheme yield more accurate results especially in the early stages of the transient radiative transfer. They also could solve the transient radiative transfer in 2D irregular geometries by using non-orthogonal mesh (which is also known as body fitted coordinates). Ruan et al. [3] used FVM to solve the TRTE in 1D homogeneous and inhomogeneous media. They found that for the two-layer media, changing in the scattering albedo and optical thickness does not alter the location of the local minimum moment. Moghadasian and Moghadassian [5] and Moghadassian and Kowsary [6] numerically investigated conjugated heat transfer problems in 2- and 3-D cavities. Kim et al. [7] applied FVM to solve TRTE in 1D slab subjected to the radiative equilibrium condition. They utilized and compared various schemes for calculating convective terms of the discretized FVM. They found that FVM is an accurate method for solving TRTE when the medium is cold or it is subjected under the radiative equilibrium condition.

One of the major difficulties in solution of RTE or TRTE is the modeling of radiative scattering. In many cases in both nature and science, there are tiny particles in media that make the scattering phenomena even more complicated. Such media is known as particulate media. Some examples are the scattering of sunshine by the atmosphere which results in blue sky, red sunset and colorful rainbow, scattering of light in interstellar dust, pulverized coal furnaces, combustion systems, etc. The most famous and general rule that governs the radiative scattering in particulate media is Mie theory that is named after Gustav Mie who solved the Maxwell equations to relate the scattering phase function to the medium properties like index of refraction and particle size. Mie theory founded a base for further studies. Some researchers in the field of radiative heat transfer have

utilized it. Trivic et al. [8,12] considered Mie scattering in the square and cubic enclosures. They successfully coupled the finite volume method (FVM) with Mie theory to perform a numerical study of the effect of anisotropic scattering on the radiative heat transfer. Steward and Trivic studied heat transfer of a convective-radiative flow [15]. They used zonal method for solving radiative heat transfer (RTE) and Mie theory for calculating the scattering phase function in a three dimensional furnace. The comparison with the experimental data showed the accuracy of their applied solution method.

In most cases, thermal engineers have preferred to use simplified relations to account radiative scattering, due to complexity of Mie theory. The Henyey-Greenstein, delta-Eddington and Legendre polynomial approximations as well as formulation of equivalent isotropic scattering are some of these relations [18].

Menguç and Viscanta [19] approximated the scattering phase function by delta-Eddington relation and solved RTE in a rectangular cube by the first and third-order spherical harmonics. In the work of Kim and Lee [20], the coupling between discrete ordinates method (DOM) and Legendre polynomial approximation was done to find the average radiative intensity and radiative heat flux in a 2D rectangular enclosure of an emitting, absorbing and anisotropically scattering medium. Guo and Kumar [21] considered a slab containing scattering media. They compared the results of applying the Henyey-Greenstein phase function with the equivalent isotropic scattering approximation. They compared the temporal distribution of transmittance and reflectance and observed that the error between the two models is more significant for the cases of backward scattering.

The aim of present study is to solve the transient radiative heat transfer in a 2D irregular geometry containing particulate media with uniform particle diameter. The TRTE is solved by FVM. The scattering phase function is calculated by applying Mie theory. The validation checks are done to make sure of the numerical code. The results are reported for media with different particle sizes, particle densities and indices of refraction. In addition, the heat transfer parameters (i.e. the heat flux and the incident irradiation) calculated by applying Mie theory are compared with those obtained by the isotropic equivalent approximation.

2. Mathematical Formulation

2.1. TRTE Solution Method

The transient radiative transfer equation in a grey, emitting, absorbing and scattering medium at any position **r** along a path **s** is given by

$$\frac{1}{c}\frac{dI(\mathbf{r},\mathbf{s})}{dt}+\frac{dI(\mathbf{r},\mathbf{s})}{ds}=-\beta I(\mathbf{r},\mathbf{s})+S(\mathbf{r},\mathbf{s}) \tag{1}$$

Where the source function can be defined as

$$S(\mathbf{r},\mathbf{s})=-\kappa I_b(\mathbf{r})+\frac{\sigma_s}{4\pi}\int I(\mathbf{r},\mathbf{s})\Phi(\mathbf{s},\mathbf{s}')\,d\Omega \tag{2}$$

The boundary condition for a diffusely emitting and reflecting wall can be written as follows

$$I(\mathbf{r}_w,\mathbf{s})=\varepsilon_w I_b(\mathbf{r}_w,\mathbf{s})+\frac{1-\varepsilon}{\pi}\int_{\mathbf{n}_w\cdot\mathbf{s}'<0} I(\mathbf{r}_w,\mathbf{s}')\left|\mathbf{n}_w\cdot\mathbf{s}'\right|d\Omega' \tag{3}$$

In the above equations I is the radiative intensity, c is the light speed in the medium; β, κ and σ_s are extinction, absorption and scattering coefficients, respectively. ε_w is the wall emissivity and Φ is the scattering phase function. The discretization process of eq. (1) is well explained in [1,2] is not repeated here.

2.2. Mie Scattering

After discretization (see [2] for example), the source term in eq. (2), can be calculated as

$$S_P^l=\kappa_P I_{b,P}+\frac{\sigma_s}{4\pi}\sum_{l'=1}^{NS}\left(I_P^{l'}\frac{\int_{\Delta\Omega^l}\int_{\Delta\Omega^{l'}}\overline{\Phi}(\mathbf{s},\mathbf{s}')\,d\Omega'\,d\Omega}{\Delta\Omega^l}\right) \tag{4}$$

If the analytical expression for scattering phase function ($\Phi(\mathbf{s},\mathbf{s}')$) exists, the average scattering phase function in eq. (8) can be obtained by the following relation

$$\overline{\Phi}(\mathbf{s},\mathbf{s}')=\frac{\int_{\Delta\Omega^l}\int_{\Delta\Omega^{l'}}\Phi(\mathbf{s},\mathbf{s}')d\Omega'\,d\Omega}{\Delta\Omega^l} \tag{5}$$

When the integration is not feasible or $\Phi(\mathbf{s},\mathbf{s}')$ is an unknown function but its value for different **s** and **s′** can be obtained, its average can be estimated by the following formula [8]

$$\overline{\Phi}(\mathbf{s},\mathbf{s}')=\frac{\sum_{l_s=1}^{L_s}\sum_{l_{s'}=1}^{L_{s'}}\Phi^{l_s,l_{s'}}\Delta\Omega^{l_s}\Delta\Omega^{l_{s'}}}{\Delta\Omega^l} \tag{6}$$

For particulate media of this study, the analytical expression for scattering phase function does not exist and therefore eq. (6) must be used. Scattering phase function in any combination of **s** and **s′** is obtained by applying Mie theory [18].

The details of complicated Mie theory are beyond the scope of this work. They may be found in the books written by van de Hulst [22] and Kerker [23]. A very compact formulation is presented subsequently.

The scattering phase function is

$$\Phi(\Psi)=2\frac{i_1+i_2}{2Q_{sca}} \tag{7}$$

The parameters of eq. (7) are

$$i_1(x_p,m,\Psi)=\left|S_1\right|^2,\quad i_2(x_p,m,\Psi)=\left|S_2\right|^2 \tag{8}$$

S_1 and S_2 are complex functions that can be expressed in terms of infinite summation of specific functions as follows

$$S_1(\Psi)=\sum_{n=1}^{\infty}\frac{2n+1}{n^2+n}\left[a_n\pi_n(\cos\Psi)+b_n\tau_n(\cos\Psi)\right]$$
$$S_2(\Psi)=\sum_{n=1}^{\infty}\frac{2n+1}{n^2+n}\left[b_n\pi_n(\cos\Psi)+a_n\tau_n(\cos\Psi)\right] \quad (9)$$

Where π and τ are related to Legendre polynomials by the following relations

$$\pi_n(\cos\Psi)=\frac{dP_n(\cos\Psi)}{d(\cos\Psi)}$$
$$\pi_n(\cos\Psi)=-\sin^2\Psi\frac{d\pi_n(\cos\Psi)}{d(\cos\Psi)}+\cos\Psi\,\pi_n(\cos\Psi) \quad (10)$$

and Mie scattering coefficients a_n and b_n are complex functions of $x_p=2\pi a_p/\lambda$ and $y_p=mx_p$.

$$a_n=\frac{\psi_n'(y_p)\psi_n(x_p)-m\psi_n(y_p)\psi_n'(x_p)}{\psi_n'(y_p)\zeta_n(x_p)-m\psi_n(y_p)\zeta_n'(x_p)}$$
$$b_n=\frac{m\psi_n'(y_p)\psi_n(x_p)-\psi_n(y_p)\psi_n'(x_p)}{m\psi_n'(y_p)\zeta_n(x_p)-\psi_n(y_p)\zeta_n'(x_p)} \quad (11)$$

Where ψ and ζ are known as Riccati-Bessel functions and can be related to Bessel and Hankel functions by

$$\psi_n(z)=\left(\frac{\pi z}{2}\right)^2 J_{n+1/2}(z)$$
$$\zeta_n(z)=\left(\frac{\pi z}{2}\right)^2 H_{n+1/2}(z) \quad (12)$$

On the other hand the Q_{sca} is also can be expressed as a function of Mie scattering coefficients as follows

$$Q_{sca}=\frac{2}{x_p^2}\sum_{n=1}^{\infty}(2n+1)\left(|a_n|^2+|b_n|^2\right)$$
$$Q_{ext}=\frac{2}{x_p^2}\sum_{n=1}^{\infty}\mathrm{Re}(a_n+b_n) \quad (13)$$

If the particles have the same size, the scattering and the extinction coefficients of the particles can be expressed as

$$\sigma_{s,\lambda}=\pi a_p^2 N_T Q_{sca}$$
$$\beta_\lambda=\pi a_p^2 N_T Q_{ext} \quad (14)$$

Although the value of x_p is dependent on wavelength, for the sake of analysis in this study, it is calculated for the typical wavelength of λ=3.1415 μm as suggested by Modest [18].

Table 1. media properties for N T=10^5 (particles/cm3) and λ=3.1415 μm (the values for index of refraction are brought from [8,18])

medium type or particle material	x_p	m (index of refractrion)	β (m^{-1})	ω	g
F1	5	1.33	1	1	0.8453
F2	2	1.33	1	1	0.6697
B1	1	108	1	1	-0.1794
B2	0.01	108	1	1	-0.4000
Carbon	2	2.20-1.12i	0.979	0.496	0.5990
Anthracite	2	2.05-0.54i	1.013	0.487	0.6549
Bituminous	2	1.85-0.22i	1.051	0.615	0.6456
Lignite	2	1.70-0.066i	0.916	0.822	0.5924
Ash	2	1.50-0.02i	0.574	0.907	0.6341
Carbon	0.5	2.20-1.12i	0.017	0.144	0.0562
Carbon	1	2.20-1.12i	0.224	0.396	0.2146
Carbon	3	2.20-1.12i	1.999	0.507	0.6997
Carbon	5	2.20-1.12i	5.172	0.542	0.7645

Table 2. Dimensionless G (=G/E_{bw}) along the centerline of the square enclosure (x=0.5 m) predicted by Kim et al. [20]

y(m)	isotropic	F1	F2	B1	B2
0.020	0.600355	0.518740	0.535868	0.616569	0.632666
0.060	0.556250	0.484921	0.498624	0.570840	0.585263
0.100	0.512708	0.449798	0.461528	0.525645	0.538400
0.140	0.474531	0.419550	0.429650	0.485822	0.496928
0.180	0.441868	0.394810	0.403170	0.451563	0.461070
0.220	0.412683	0.373385	0.379963	0.420857	0.428843
0.260	0.385379	0.353413	0.358333	0.392118	0.398681
0.300	0.359364	0.334146	0.337640	0.364761	0.369998
0.340	0.334617	0.315545	0.317857	0.338761	0.342773
0.380	0.311256	0.297782	0.299127	0.314241	0.317122
0.420	0.289369	0.281022	0.281556	0.291279	0.293117
0.460	0.268964	0.265367	0.265191	0.269885	0.270764
0.500	0.249999	0.250859	0.250021	0.250002	0.249999
0.540	0.232387	0.237473	0.235981	0.231539	0.230725
0.580	0.216013	0.225155	0.222990	0.214376	0.212815
0.620	0.200763	0.213820	0.210952	0.198395	0.196136
0.660	0.186516	0.203371	0.199764	0.183463	0 180560
0.700	0.173155	0.193714	0.189331	0.169461	0.165955
0.740	0.160570	0.184751	0.179558	0.156275	0.152204
0.780	0.148657	0.176397	0.170359	0.143791	0.139191
0.820	0.137300	0.168568	0.161635	0.131900	0.126801
0.860	0.126371	0.161186	0.153281	0.120471	0.114907
0.900	0.115699	0.154161	0.145179	0.109337	0.103343
0.940	0.105067	0.147404	0.137162	0.098291	0.091917
0.980	0.094238	0.140816	0.129025	0.087135	0.080447

In addition, the evolution of infinite series in the above equation is terminated by the following relation of Deirmendjian et al. [24].

$$n = 9 + 1.2x_p \tag{15}$$

There are recursive formulae and series for calculation of the Bessel and Hankel as well as Legendre polynomials and their derivatives [24] that are used in this study to write the numerical FORTRAN 90 code.

2.3. Equivalent Isotropic Approximation

The equivalent scattering and extinction coefficients as well as the equivalent single scattering albedo can be related to the original values according to the following relations [21],

$$\sigma_{s,eq} = (1-g)\sigma_s \tag{16}$$

$$\beta_{eq} = \kappa + \sigma_{s,eq} = (1-g\omega)\beta \tag{17}$$

$$\omega_{eq} = \frac{\sigma_{s,eq}}{\beta_{eq}} = \frac{(1-g)\omega}{(1-g\omega)} \tag{18}$$

where the dimensionless asymmetry factor is

$$\frac{1}{c}\frac{dI(\mathbf{r},\mathbf{s})}{dt} + \frac{dI(\mathbf{r},\mathbf{s})}{ds} = -\beta I(\mathbf{r},\mathbf{s}) + S(\mathbf{r},\mathbf{s}) \tag{19}$$

and $\gamma=cos\ \Psi$.

The integration of eq. (19) is calculated numerically using the trapezoid rule with 1000 points in the range of $-1 \le \gamma \le 1$.

3. Validation Check

First the numerical code for the Mie scattering is validated by the results of Trivic et al. [8] and Kim et al. [20]. Consider a square enclosure of length $L=1\ m$. The bottom wall is black and hot ($E_{b,ref}=1\ W/m2$) and other walls are cold and black at $0K$. The medium is purely scattering with $\beta=1\ m^{-1}$. The indices of refraction are assumed real and are brought in Table 1. Trivic et al. [8] and Kim et al. [20] considered this problem but just the results of Kim et al. [20] are brought here for the sake of brevity. Their predicted values for $G/E_{b,ref}$ along the centerline of enclosure ($x=0.5\ m$) are reported in Table 2. The results of this study are brought in Table 3. The identical 25×25 spatial grid is used for better point-to-point comparison. The $L_s=3\times3$ is used as suggested in [8]. The finer sub-control angle is seen to produce insignificant difference in results.

In addition, the numerical code is checked for the cases of complex indices of refraction of Table 1. The scattering phase function for different values of Ψ ($0 \le \Psi \le \pi$) is obtained and is shown in Figure 1a and Figure 1b. They are exactly the same as the diagrams obtained by Trivic et al. [12] that are not shown here.

Table 3. Dimensionless G (=G/E$_{bw}$) along the centerline of the square enclosure (x=0.5 m) predicted in this study.

y(m)	isotropic	F1	F2	B1	B2
0.020	0.599530	0.519407	0.536840	0.614522	0.630658
0.060	0.559019	0.490733	0.503624	0.572443	0.586791
0.100	0.515640	0.456089	0.466700	0.527509	0.540154
0.140	0.473927	0.421347	0.430908	0.484273	0.495285
0.180	0.436937	0.390839	0.399591	0.445811	0.455250
0.220	0.405248	0.365777	0.373455	0.412717	0.420652
0.260	0.377859	0.345202	0.351482	0.384006	0.390520
0.300	0.353372	0.327464	0.332195	0.358285	0.363474
0.340	0.330672	0.311171	0.314405	0.334444	0.338408
0.380	0.309122	0.295505	0.297435	0.311840	0.314682
0.420	0.288479	0.280168	0.281038	0.290226	0.292042
0.460	0.268740	0.265196	0.265231	0.269591	0.270468
0.500	0.250000	0.250780	0.250147	0.250024	0.250039
0.540	0.232367	0.237142	0.235934	0.231623	0.230846
0.580	0.215911	0.224465	0.222704	0.214453	0.212941
0.620	0.200647	0.212856	0.210506	0.198524	0.196327
0.660	0.186538	0.202348	0.199332	0.183790	0.180954
0.700	0.173501	0.192906	0.189123	0.170165	0.166726
0.740	0.161418	0.184443	0.179782	0.157526	0.153516
0.780	0.150144	0.176839	0.171188	0.145724	0.141172
0.820	0.139512	0.169950	0.163200	0.134587	0.129517
0.860	0.129330	0.163622	0.155661	0.123922	0.118357
0.900	0.119384	0.157694	0.148394	0.113519	0.107482
0.940	0.109454	0.152000	0.141198	0.103167	0.096693
0.980	0.099330	0.146370	0.133846	0.092687	0.085831

Then the ability of the code is examined for the case of non-orthogonal mesh. The transient radiative heat transfer in 2D quadrilateral enclosure of Figure 2a is considered. The enclosure is filled with an emitting, absorbing and non-scattering medium at T_{ref}. The 25×25 grid system is shown in Figure 2a. All walls are black at T_w=0K. The extinction coefficient is 1 m^{-1}. The characteristic time step is $\Delta t_c=h/400c$ where h=1 m for this case. It is found that further decrease in Δt_c does not change the results significantly. The dimensionless radiative heat flux on the

bottom wall is compared with previously published results of Chai et al. [10]. The comparison is shown in Figure 2b.

As it can be seen in all cases a good agreement between the results of present study and previously reported ones is seen. This can secure the accuracy of the results of subsequent sections.

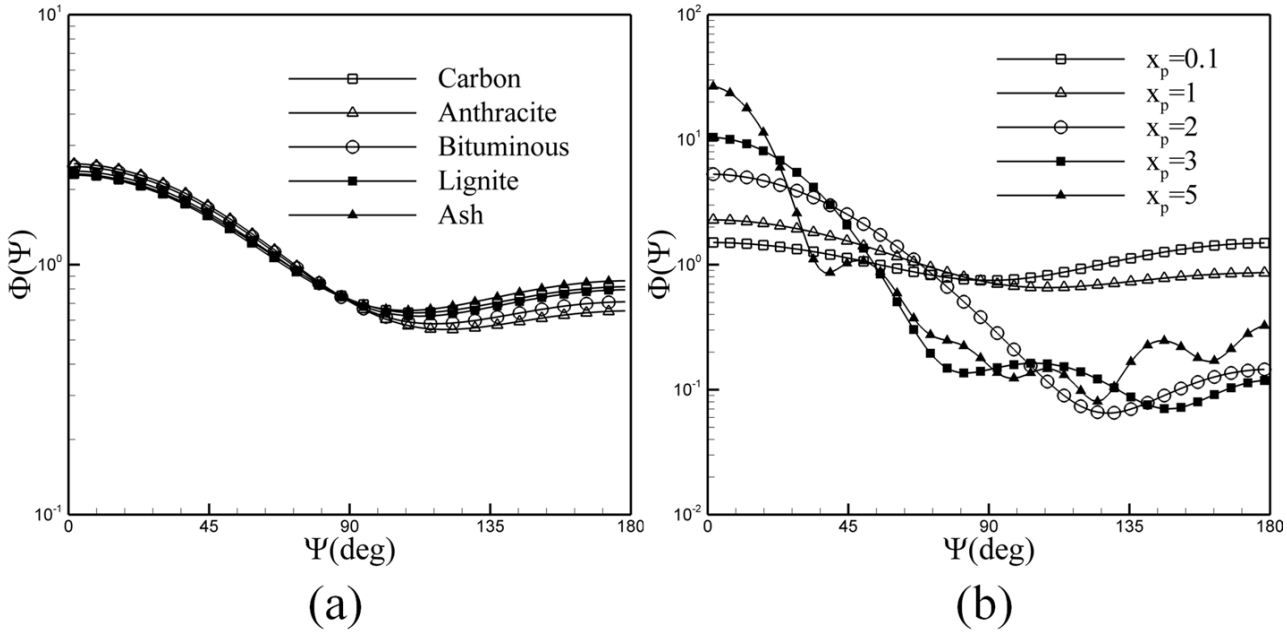

Figure 1. Scattering phase function for (a) different materials of Table 1 at x_p=1 and (b) for Ash at different particle size parameters

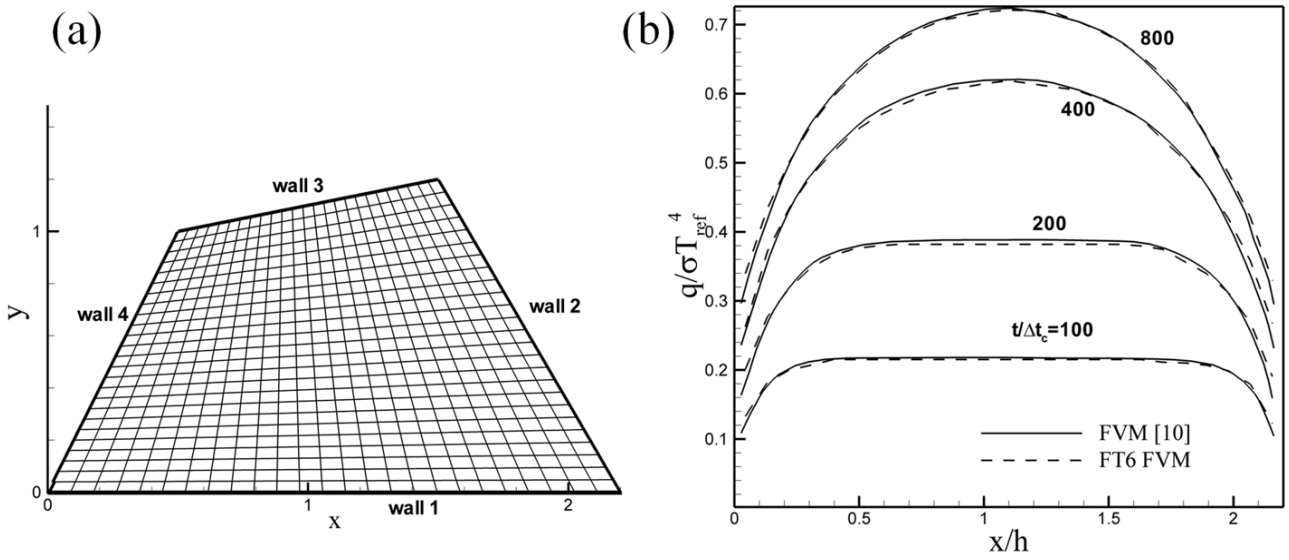

Figure 2. The validation check for FT6 FVM with non-orthogonal grid (a) the geometry and grid and (b) the dimensionless heat flux on the bottom wall

4. Results and Discussions

The transient radiative heat transfer is numerically investigated in a quadrilateral of Figure 2a. It should be stated that the radiative equilibrium condition is applied to all cases. All the walls are black. The wall number 3 is hot ($E_{b,ref}=\sigma T_{ref}^4$=1 W/m^2). Other walls are cold at 0K. The medium is initially at 0K. The characteristic time step is $\Delta t_c=h/400c$.

First the dielectric particles (those with real index of refraction) of Table 1 in medium with $\beta=1$ m^{-1} are considered. For the sake of analysis, the medium is assumed purely scattering and eq. (14) is not used to find the values of β and σ_s.

The temporal dimensionless heat flux on the bottom wall of Figure 2a is illustrated in Figure 3a and Figure 3b for F1 and B2. It is seen that for forward scattering medium, in each time step the heat flux on the bottom surface is higher because the value of radiative intensity is larger in comparison with backward scattering. In these figures Mie calculations are compared with the equivalent isotropic approximation. It should be noted that both of the media are assumed purely scattering. It is seen that the equivalent isotropic approximation underpredicts the radiative flux for backward scattering medium and overpredicts it for forward scattering medium. The reason is that the equivalent optical thickness is higher than the original value for the backward scattering. Therefore the medium absorbs greater amount of energy and weaker

radiative intensity reaches at the cold surface. Conversely, the equivalent optical thickness is lower than the original value for forward scattering. The maximum relative difference between the results of the equivalent isotropic approximation and those of Mie theory is 9.0% which happens for B2 at $t/\Delta t_c=600$. The maximum relative difference for the steady state results ($t/\Delta t_c=800$) is 3.6%.

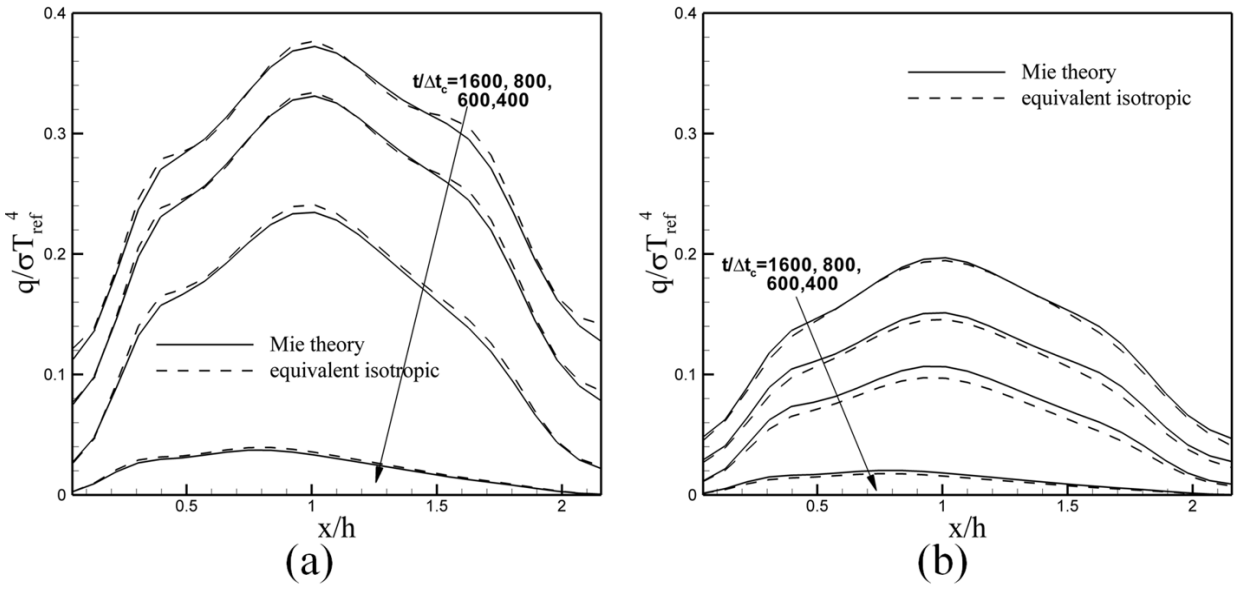

Figure 3. The temporal dimensionless heat flux on the bottom wall for (a) F1 (the forward scattering medium) and (b) B2 (the backward scattering medium)

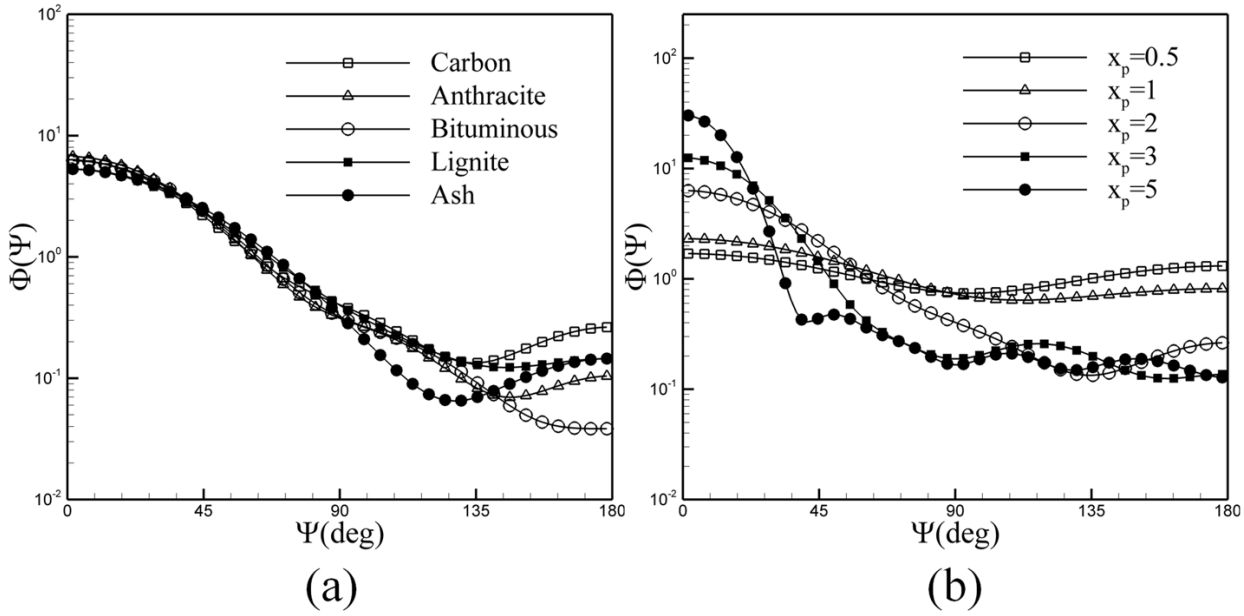

Figure 4. The scattering phase function for (a) different materials of Table 1 at x_p=2 and (b) for carbon particles at different size parameters

Then the absorbing particles (those with complex index of refraction) of Table 1 Are considered. The particle density is $N_T=10^5$ particles/cm^3. The scattering phase function for different materials at $x_p=2$ is shown in Figure 4a. The scattering phase function for different sizes of the carbon particles is also shown in Figure 4b. It is easily noticed that all particles have the forward scattering character because their scattering phase functions have higher values for acute angles of scattering. The peak of the function happens at Ψ=0. This forward characteristic becomes more significant for higher size parameters as can be seen in Figure 4b where the peak of the scattering phase function at Ψ=0 becomes more pronounced at higher values of x_p.

Figure 5 shows the dimensionless radiative flux on the bottom surface. As shown in this figure, the difference in the scattering phase function for various particles is not much. Therefore the difference in the values of radiative flux of Figure 5 is mainly attributed to the values of β and ω. Besides the fact that the radiative intensity travels with lower changes in a media with lower extinction coefficient, the value of single scattering albedo has a significant impact on radiative transfer. In cold regions such as neighborhood of the bottom wall, the first term on the right of eq. (4) tends to zero and the source term reduces. But the nodal coefficient (a_P) remains unchanged. Therefore the ratio of σ_s to β becomes important and higher ω leads to higher radiative intensity. As a result the

heat flux in a medium such as ash with lower value of β and higher value of ω must be stronger.

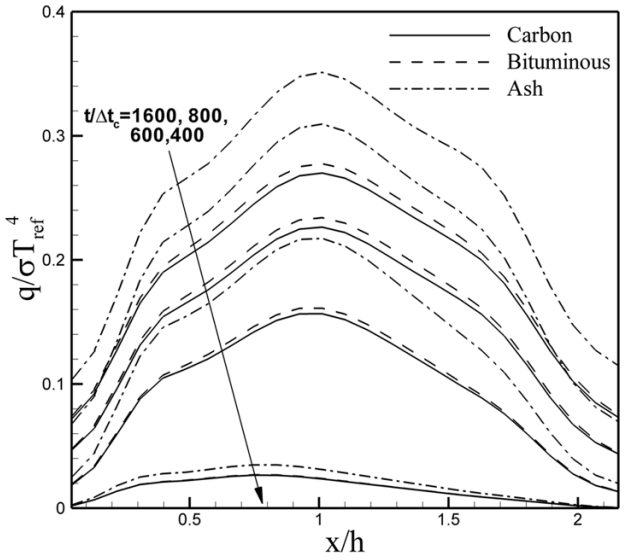

Figure 5. The temporal dimensionless heat flux on the bottom surface for different particulate media

Another noticeable issue in Figure 5 is the influence of cold walls on the radiative heat flux of the bottom wall. The heat flux is low at smaller values of x because this region of wall 1 sees more of wall 4 that is a cold wall.

When x/h increases, the influence of wall 4 diminishes and in the midsection of the bottom wall (around $x/h=1$), the heat flux reaches its peak under the influence of hot wall 3. Then due to the presence of another cold wall (wall 2) the decrement of q starts and at the end of the bottom wall, it again reaches minimum.

The comparison of Mie calculations with the equivalent isotropic approximation for media of carbon and lignite particles is displayed in Figure 6a and Figure 6b, respectively. Again the heat flux is slightly overpredicted by the equivalent isotropic approximation. The larger relative difference between Mie theory and the equivalent isotropic calculations is 4.3% which occurs for lignite particles at $t/\Delta t_c=600$. The maximum difference has reduced since in these cases the medium is not purely scattering and by using the equivalent approximation the optical thickness does not change as significant as in the cases of a purely isotropic medium. Also this difference is larger for medium containing lignite particles because it has a higher ω as reported in Table 1. As a result, applying isotropic approximation changes its equivalent β and ω more abruptly relative to the media such as carbon particles that have lower value of ω.

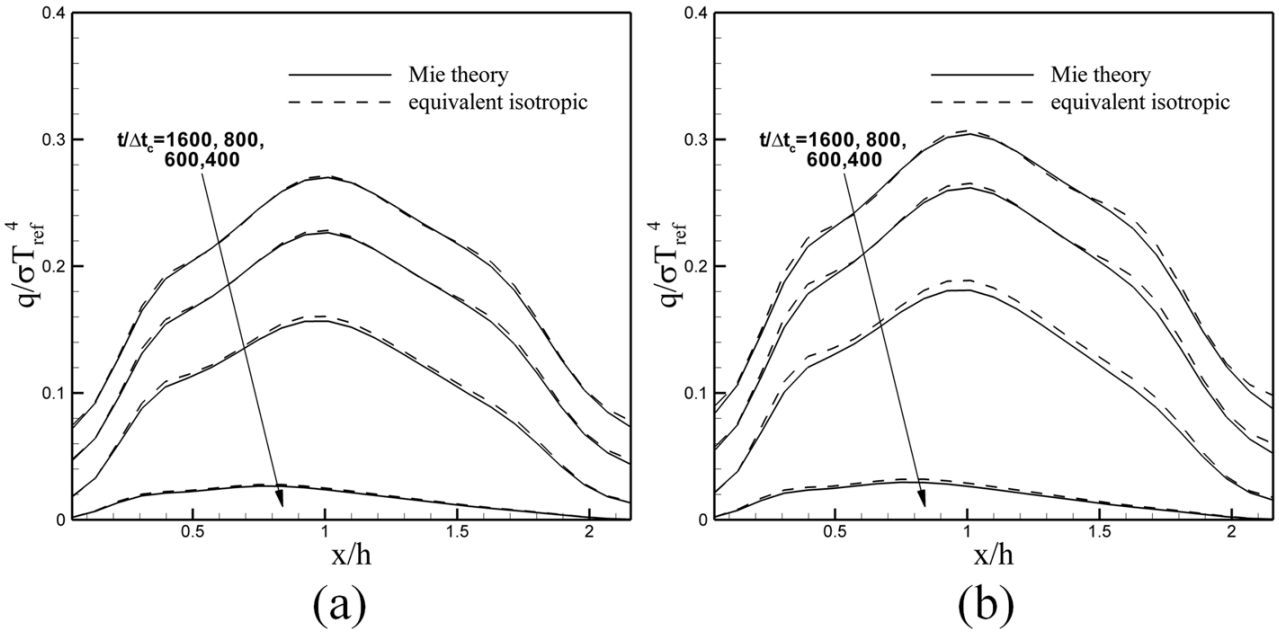

Figure 6. The temporal dimensionless heat flux on the bottom wall for media of (a) carbon particles and (b) lignite particles

5. Conclusions

In this work the transient radiative heat transfer in particulate media with the radiative equilibrium condition is considered. The solution is performed numerically by coupling of Mie theory and FVM with CLAM scheme. It is assumed that the medium itself (without the particles) does not participate in radiative transfer. After validating the code, different types of media are considered. In addition, the results of applying Mie theory are compared with the equivalent isotropic approximation. Based on the results, some conclusions can be drawn:

- Radiative heat flux on the cold surface is higher for forward scattering media;
- The transient and steady state temperature fields tend to be more uniform for forward scattering;
- At a constant particle diameter ash particles have the highest value of ω among absorbing particles because they have the lowest absorptive index among other materials of Table 1 and radiative flux is higher for medium of fly ash particles;
- The effect of cold walls is important in predicted values of heat flux;
- The equivalent isotropic approximation underpredicts the heat flux on the cold surface for

the backward scattering medium. It overpredicts the heat flux for the forward scattering medium;

- The radiative flux and integrated intensity are higher for media with smaller particles;
- The equivalent isotropic approximation is much simpler than the Mie theory and its predictions are accurate especially in the cases of forward scattering and absorbing particles. Also it is more accurate for the steady state solutions than the transient ones. However, its key parameter, g, is found when Φ is obtained. Therefore an analytical expression or numerical data of Φ is required.

References

[1] Chai, J.C., "One-dimensional transient radiation heat transfer modeling using a finite-volume method," *Numer Heat Transfer B*, 44, 187-208, 2003.

[2] Chai, J.C., Hsu, P-f. and Lam, Y.C., "Three-dimensional transient radiative transfer modeling using the finite-volume method," *J Quant Spectrosc Radiat Transfer*, 86, 299-313, 2004.

[3] Ruan, L.M., Wang, S.G., Qi, H. and Wang, D.L., "Analysis of the characteristics of time-resolved signals for transient radiative transfer in scattering participating media," *J Quant Spectrosc Radiat Transfer*, 111, 2405-14, 2010.

[4] Moghadassian, B., Kowsary, F. and Gholamian, H., "Natural convection-radiation heat transfer in rectangular cavity with the presence of participating Media," *ASME 2010 10th Biennial Conference on Engineering Systems Design and Analysis. American Society of Mechanical Engineers*, 2010.

[5] Moghadasian, M. and Moghadassian, B., "3 D inverse boundary design problem of conduction-radiation heat transfer," *Journal of Applied Sciences(Faisalabad)*, 12(3), 233-243, 2012.

[6] Moghadassian, B. and Kowsary, F., "Inverse boundary design problem of natural convection–radiation in a square enclosure," *International Journal of Thermal Sciences* 75, 116-216, 2014.

[7] Kim, M.Y., Menon, S. and Baek, S.W., "On the transient radiative transfer in a one-dimensional planar medium subjected to radiative equilibrium." *Int J Heat Mass Transfer*, 53, 5682-91, 2010.

[8] Trivic, D.N., O'Brien, T.J. and Amon, C.H., "Modeling the radiation of anisotropically scattering media by coupling Mie theory with finite volume method," *Int J Heat Mass Transfer*, 47, 5765-80, 2004.

[9] Kowsary, F., Gholamian, H. and Moghadassian, B., "On the sensitivity of surface reflectance to specularity and phase function parameters in MPA modeling of radiative transfer in two-component media," *Numer Heat Transfer B*, 2015.

[10] Chai, J.C., "Transient radiative transfer in irregular two-dimensional geometries," *J Quant Spectrosc Radiat Transfer*, 84, 281-94, 2004.

[11] Moghadassian, B., Kowsary, F. and Mosavati, M., "The radiative boundary design of a hexagonal furnace filled with gray and nongray participating gases," *Journal of Thermal Science and Engineering Applications* 5(3), 031005, 2013.

[12] Trivic. D.N. and Amon, C.H., "Modeling the 3-D radiation of anisotropically scattering media by two different numerical methods," *Int J Heat Mass Transfer*, 51, 2711-32, 2008.

[13] Razi, P., Moghadassian, B. and Shokouhmand, H., "The effect of conductive and non-conductive flow diverters on free convection heat transfer from a vertical array of horizontal isothermal cylinders," *ASME 2009 Heat Transfer Summer Conference collocated with the InterPACK09 and 3rd Energy Sustainability Conferences. American Society of Mechanical Engineers*, 2009.

[14] Moghadassian, B., Razi. P. and Shokouhmand, H., "Investigating double diffusive convection in an inclined rectangular porous enclosure subjected to magnetic field," *ASME 2009 Heat Transfer Summer Conference collocated with the InterPACK09 and 3rd Energy Sustainability Conferences. American Society of Mechanical Engineers*, 2009.

[15] Steward, F.R. and Trivic, D.N., "An assessment of particle radiation in a pulverized-coal-fired boiler," *J Inst Energy*, 452, 138-46, 1989.

[16] Jafari, A., Rahimian M.H. and Saeedmanesh. A., "An unsteady mixed convection in a driven cavity filled with nanofluids using an externally oscillating lid." *Journal of Electronics Cooling and Thermal Control* 3.02, 58, 2013.

[17] Shokouhmand, H., Noori Rahim Abadi S.M.A., and Jafari, A., "The effect of the horizontal vibrations on natural heat transfer from an isothermal array of cylinders." *International Journal of Mechanics and Materials in Design* 7.4, 313-326, 2011.

[18] Modest, M.F., *Radiative Heat Transfer*. 2nd ed. Academic Press, New York, 2003.

[19] Mengüç, M.P. and Viscanta, R., "Radiative transfer in three-dimensional rectangular enclosures containing inhomogeneous anisotropically scattering media," *J Quant Spectrosc Radiat Transfer*, 33, 533-49, 1985.

[20] Kim, T.K. and Lee, H., "Effect of anisotropic scattering on radiative heat transfer in two-dimensional enclosures" *Int J Heat Mass Transfer*, 31, 1711-21, 1988.

[21] Guo, Z. and Kumar, S., "Equivalent isotropic scattering formulation for transient short-pulse radiative transfer in anisotropic scattering planar media," *Appl Optics*, 39, 4411-17, 2000.

[22] Van de Hulst, H.C., *Light scattering by small particles*, Dover publications, New York, 1981.

[23] Kerker, M., *The scattering of light and other electromagnetic radiation*, Academic Press, New York, 1969.

[24] Deirmendjian, D., Clasen, R. and Viezee, V., "Mie scattering with complex index of refraction," *J Opt Soc Am*, 51, 620-633, 1961.